

Magnetohydrodynamic equilibrium and stability of rotating fieldreversed configurations with excluded multipole fields

R. L. Spencer and M. Tuszewski

Citation: *Physics of Fluids (1958-1988)* **28**, 2510 (1985); doi: 10.1063/1.865259

View online: <http://dx.doi.org/10.1063/1.865259>

View Table of Contents: <http://scitation.aip.org/content/aip/journal/pof1/28/8?ver=pdfcov>

Published by the [AIP Publishing](#)

Articles you may be interested in

[Rotational stability of a long field-reversed configuration](#)

Phys. Plasmas **21**, 022506 (2014); 10.1063/1.4865409

[Equilibrium rotation in field-reversed configurations](#)

Phys. Plasmas **15**, 012505 (2008); 10.1063/1.2834271

[Stability of equilibrium in rotating magnetic field current drive for sustaining field-reversed configuration](#)

Phys. Plasmas **9**, 2633 (2002); 10.1063/1.1472504

[Linear gyroviscous stability of field-reversed configurations with static equilibrium](#)

Phys. Plasmas **8**, 1240 (2001); 10.1063/1.1354645

[Magnetohydrodynamic equilibrium and stability of fieldreversed configurations](#)

Phys. Fluids **26**, 1295 (1983); 10.1063/1.864290



HAVE YOU HEARD?

Employers hiring scientists
and engineers trust
physicstodayJOBS



<http://careers.physicstoday.org/post.cfm>

Magnetohydrodynamic equilibrium and stability of rotating field-reversed configurations with excluded multipole fields

R. L. Spencer^{a)} and M. Tuszewski

University of California, Los Alamos National Laboratory, Los Alamos, New Mexico 87545

(Received 9 August 1984; accepted 5 April 1985)

The rotational instability in field-reversed configurations (FRC's) is observed experimentally to be suppressed by the application of multipole fields. In this paper the equilibrium and stability of a FRC with multipole fields that do not penetrate into the plasma are studied. It is shown that two rotating magnetohydrodynamic (MHD) equilibria are possible for a long FRC in a multipole field. One is nearly circular while the other is cusp shaped. Experiments and hybrid simulations indicate that cusp-like equilibria are usually obtained. The effect of helical multipole fields on the equilibrium is also discussed. The stability of such a configuration has been previously studied by using the MHD model on a circular plasma and by using a hybrid simulation code. In the important quadrupole case, the two calculations disagree: the simulation shows that the mode is stabilized while the circular MHD calculation predicts that it remains unstable. A close look at the MHD calculation shows that stability is strongly influenced by the shape of the equilibrium. Simple estimates indicate that the cusp-like equilibrium should be more stable than the circular one.

I. INTRODUCTION

A recurring problem in the study of field-reversed configurations (FRC's) has been the onset of an $n = 2$ rotational instability that eventually grows to such large amplitude that the plasma strikes the wall and rapidly dissipates. Recently, it was found experimentally that the application of multipole fields can suppress this instability.¹⁻⁴ This effect was first studied theoretically in the magnetohydrodynamic (MHD) model in a simple circular geometry⁵ where it was found that quadrupole fields essentially do not stabilize the $n = 2$ rotational mode because of mode coupling. This is in conflict with hybrid simulations of FRC's with applied quadrupole fields in which stabilization was observed.⁶ In this paper the disagreement between these two calculations is shown to be caused by the assumption of a circular plasma shape in the MHD calculation. In Sec. II it is shown that there are two classes of FRC equilibria with excluded multipole fields: quasicircular equilibria, similar to those considered in Ref. 5, and cusp equilibria. Simple dynamical considerations as well as results from experiments³ and simulations^{6,7} show that cusp-like equilibria are usually obtained. In Sec. III the stability calculation of Ref. 5 is reexamined to see what the effect of a noncircular plasma might be. It is found that the mode-coupling problem in the case of quadrupole fields is very delicate and depends crucially on equilibrium details. Modifying the circular result to take into account some of the features of a cusp-shaped equilibrium can stabilize the rotational mode, in rough agreement with experiments and hybrid simulations. In Sec. IV the paper is briefly summarized and the agreement between theory and experiment is discussed. In the Appendix the effect of helical multipole fields is briefly discussed.

^{a)}New address: Department of Physics and Astronomy, Brigham Young University, Provo, Utah 84602.

II. EQUILIBRIUM

A sketch of a circular FRC with an excluded quadrupole field is shown in Fig. 1. (Note that a rotating FRC will tend to exclude the multipole fields because the flow will shear the field lines off in a skin depth. Also, note that in this and in the following sections it will be assumed that the FRC is infinitely long.) The multipole fields will, of course, distort the shape of the surface, but basically it has been previously assumed that the FRC has a more or less circular shape with multipole field nulls occurring along the plasma surface. Making this assumption, a qualitative description of the shape of the perturbed plasma surface can be obtained by using Bernoulli's law. When the flow is in a plane perpendicular to a set of straight field lines, Bernoulli's law states that

$$\frac{u^2}{2} + \frac{\gamma(\gamma - 1)p}{\rho} + \frac{B^2}{\mu_0\rho} = \text{const on streamlines}, \quad (1)$$

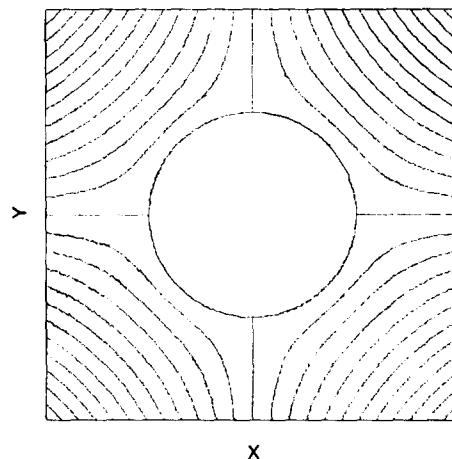


FIG. 1. A flux plot of a multipole field that is excluded by a cylindrical conductor and whose sources are at infinity is displayed. Note the bad curvature near the conductor surface.

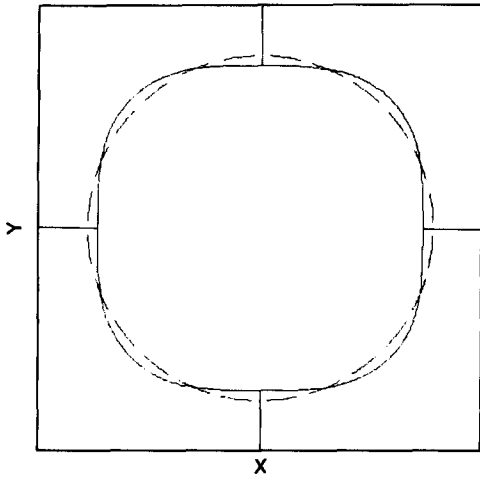


FIG. 2. For an equilibrium of the kind discussed in Ref. 5 the deviation from the original circular shape is displayed by the solid line. The straight lines are the separatrices of the multipole field.

where u is the fluid speed, γ is the adiabatic exponent, p is the fluid pressure, ρ is the fluid density, and B is the axial magnetic field strength. There are two other quantities that are invariant along streamlines, namely p/ρ^γ and B/ρ . (In what follows it will be assumed that $\gamma = 2$, as is appropriate for a system with two degrees of freedom. Relaxing this assumption does not qualitatively change the results derived here.) By combining these three laws, an expression for the total pressure along a streamline as a function of the fluid speed can be derived:

$$p + B^2/2\mu_0 \propto (\text{const} - u^2)^2. \quad (2)$$

This equation must be satisfied at the fluid–vacuum interface since it is a streamline. Also, the total pressure must be balanced by the magnetic pressure on the other side of the interface. Hence where the external magnetic pressure is low, the fluid speed must be high, and vice versa. But the fluid velocity will be low where the surface bulges out and



FIG. 3. An end-on hologram of the plasma in FRX-C is displayed.³ The external multipole field is oriented as in Fig. 1.

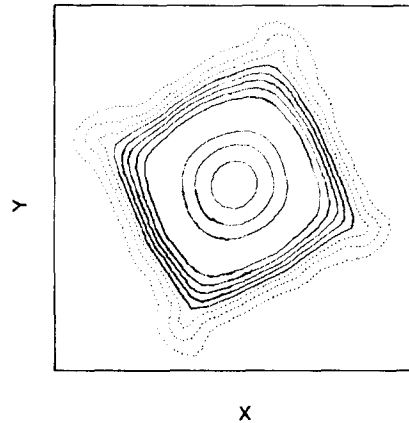


FIG. 4. Density contours from a two-fluid simulation⁷ of a FRC with the external multipole field oriented as in Fig. 1 are displayed. The fluid is rotating in the clockwise direction.

high where it bulges in (think about two-dimensional flow around outward- and inward-pointing corners), so the following general statement can be made: A rotating FRC equilibrium that excludes a multipole field such that multipole field nulls occur on the fluid–vacuum interface must bulge out where the external magnetic pressure is high and bulge in at the field null, as shown in Fig. 2. There is one other property of equilibria of this type that follows from these arguments. Since the pressure variation must be produced by a variation in the flow speed, if the flow speed is too low, there will be no equilibria. That is, equilibria of this type are nearly circular at very high values of the rotation velocity, but as this velocity is reduced the boundary becomes more and more distorted until finally different parts of the boundary touch one another and equilibrium is lost.

An example of an equilibrium of this type with exactly these properties is presented in Sec. IV of Ref. 5. There the distortion is called a forced oscillation, but that is only because the calculations in Ref. 5 are performed in a rotating frame. If all quantities are transformed back into the lab frame, the time dependence disappears and an equilibrium distortion like that shown in Fig. 2 appears. In Ref. 5 an estimate is made, using a linear calculation, of the condition on the rotation frequency for an equilibrium to exist: $\Omega r_s > B_m/(\mu_0 \rho)^{1/2}$, where B_m is the peak multipole field on the fluid surface, Ω is the rotation frequency, and r_s is the plasma radius. This requires that the rotational energy density exceed the multipole magnetic energy density.

However, experiments and simulations do not show equilibrium distortions of the kind described above. Instead, the distortions are rotated by $\pi/4$ from those shown in Fig. 2. Figure 3 shows an end-on hologram of a quadrupole stabilized FRC in the FRX-C device at Los Alamos³ and Fig. 4 shows density contours from a two-fluid simulation⁷ (the slight rotation from vertical orientation is probably the result of not running the program long enough for transient effects to have died away). To understand how such configurations come to be, imagine a circular FRC to which multipole fields have just been applied. A configuration like that shown in Fig. 1 will be produced, but it will not be in equilibrium. The excess magnetic pressure on the surface between the field nulls will push the surface in and begin to make a distortion like that shown in Figs. 3 and 4. But by the pre-

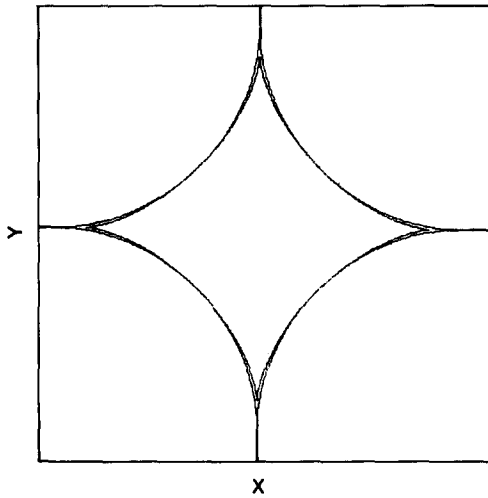


FIG. 5. Two cusp shapes are displayed. The inner one is the usual hypocycloid cusp with $|\mathbf{B}| = \text{const}$ on the surface [$\sigma = \frac{1}{3}$ in Eqs. (3-4)]. The outer one has $|\mathbf{B}|$ at the cusp tip 40% higher than $|\mathbf{B}|$ halfway between the tips ($\sigma = 0.42$).

vious arguments, there cannot be an equilibrium of this kind as long as there are multipole field nulls on the surface. The surface will continue to be pushed in until the field nulls can somehow be replaced by points of maximum magnetic pressure instead of minimum magnetic pressure. Fortunately, such a state can be achieved; the field null region becomes more and more pointed until the field null simply disappears and the fluid surface takes the shape of a cusp, as shown in Fig. 5. The usual definition of a free-boundary cusp is that it is a configuration in which the surface magnetic field is constant. This is not required, however, and cusps, for which the surface magnetic field is stronger at the cusp tips than it is between them, are easily obtained by modifying the conformal mappings that give the constant $|\mathbf{B}|$ cusp.⁸ The inner cusp in Fig. 5 is the standard hypocycloid cusp shape given by $x^{2/3} + y^{2/3} = \text{const}$,⁹ while the outer one has a surface magnetic field at the tip that is 40% higher than the field midway between the tips.

The nonconstant $|\mathbf{B}|$ cusp can be represented parametrically as follows:

$$F(\omega) = \phi + i\psi = B_0 r_0 \cos(2\omega),$$

$$z(\omega) = x + iy = r_0 \exp(i\omega) \sum_{m=0}^{\infty} a_m \exp(-i4m\omega), \quad (3)$$

$$\mathbf{B}(\omega) = B_x - iB_y = \frac{dF}{dz},$$

where $\omega = \omega_r + i\omega_i$ is a complex variable in the range $0 < \omega_r < 2\pi$ and $-\infty < \omega_i < 0$. The quantity ϕ is the magnetic potential, ψ is the magnetic stream function, B_0 is a characteristic magnetic field value on the cusp surface, and r_0 is a characteristic radius. The sum for $z(\omega)$ has the form given because we require that the magnetic field at infinity be a quadrupole field and because we require quadrupole symmetry. If $\omega_i = 0$, then ω_r parametrizes the cusp surface. Note that $\omega = 0, \pi/2, \pi$, and $3\pi/2$ correspond to the cusp tips while $\omega = \pi/4, 3\pi/4, 5\pi/4$, and $7\pi/4$ correspond to the midpoints between cusp tips. For the above expressions to

correspond to a cusp, it is necessary that $dz/d\omega = 0$ at $\omega = 0$, i.e., that $\sum_{m=0}^{\infty} a_m (1 - 4m) = 0$. This condition is only necessary; some choices for the a_m that satisfy it may yield shapes other than cusps, e.g., shapes with loops where a cusp tip should be. The simplest example of a nonconstant $|\mathbf{B}|$ cusp is obtained by choosing $a_0 = 1$, $a_1 = \sigma$, and $a_2 = (1 - 3\sigma)/7$, where σ is an adjustable parameter. Note that $\sigma = \frac{1}{3}$ gives the hypocycloid cusp. The complex magnetic field on the surface for this case is given by

$$\mathbf{B} = B_x - iB_y,$$

$$= B_0 / [2 \exp(-i3\omega) \cos 2\omega - 3\sigma \exp(-i5\omega)]. \quad (4)$$

As σ is increased from the value $\frac{1}{3}$, the magnetic field at the cusp tips becomes greater than the field midway between the tips. The tip field is 40% greater than the midpoint field when $\sigma = 0.42$. (If σ is increased further, the cusp tip changes into a loop.) This is enough variation to account for most situations of experimental interest. This cusp shape is not the result of a self-consistent equilibrium calculation, however. To actually find an equilibrium of this kind it would be necessary to include many terms in the sum for $z(\omega)$ and then to determine the coefficients by solving for the flow inside the cusp. This will, of course, be hard. Note from Fig. 5 that there is very little distortion of the cusp even for substantial amounts of field variation, and hence for fairly large flow speeds. Note also that there is no loss of equilibrium at low flow speeds; the state with no flow must have constant $|\mathbf{B}|$ and is hence simply the hypocycloid cusp.

Therefore, there are at least two kinds of rotating FRC equilibria with flow: (1) quasicircular equilibria with the surface bulging outward in regions of maximum multipole field and having multipole field nulls on the surface, and (2) cusp equilibria with more or less constant multipole magnetic field at the fluid surface. Both of these equilibria are idealizations; fine details like cusp tips will not be observed in experiments. Experiments and simulations suggest, however, that cusp-like equilibria are usually observed.

III. STABILITY

The rotational instability in FRC's has been studied⁵ using the state shown in Fig. 1. This work probably gives approximate information about an equilibrium like that indicated in Fig. 2. The best-known result from this paper is that the mode is stable when

$$B_m > D r_s \Omega (\mu_0 \rho)^{1/2}, \quad (5)$$

where D is a constant of order one $\{D^2 = 2(n-1)/n[\max(n, m) - 1]\}$, n is the mode number, and $m = 2$ for quadrupole fields, $m = 3$ for hexapole fields, etc. This result seems quite robust. It states, roughly, that stability is achieved when the average rotational energy density of the fluid is equal to the average energy density of the multipole field at the plasma surface. It assumes that the multipole coils are at infinity and that in the equilibrium $\gamma p + B^2/\mu_0$ is constant. Relaxing these restrictions to include the effect of coils at a finite radius, a conducting wall, and a realistic equilibrium profile only slightly reduces the right-hand side of

Eq. (5) (by 25% for the parameters³ of FRX-C). But the careful analysis of Ref. 5 shows that this simple result is not always valid. In particular, in the case of the $n = 2$ mode and quadrupole fields, mode coupling induced by the $n = 4$ ripple of the quadrupole pressure makes the $n = 2$ and $n = 6$ modes strongly interact to give essentially no stabilization. A closer look at the reasons for this curious result reveals that it depends crucially on the kind of equilibrium used.

The state shown in Fig. 1 has an important special feature; in spite of the generally stabilizing influence of the multipole field, the curvature is bad at the surface. This means that when the perturbed magnetic field pressure caused by a displacement of the surface is computed, one of the terms that results is destabilizing. This destabilizing term plays a critical role in the mode coupling that occurs in the $n = 2$ quadrupole field case. To make this clear, a few of the equations from Ref. 5 will be given here. The equations that determine the eigenfrequencies are

$$AG_{k-1} C_{k-1} - (E_k - AF_k) C_k + AH_{k+1} C_{k+1} = 0, \quad (6)$$

where $A = B_m^2 / 4\mu_0 \rho r_s^2 \Omega^2$ and the C_k 's are the coefficients in the mode expansion of the radial displacement, ξ_r :

$$\frac{A^2 G_{-1} H_0}{(E_{-1} - AF_{-1}) - \frac{A^2 G_{-2} H_{-1}}{(E_{-2} - AF_{-2}) - \dots}} - (E_0 - AF_0) + \frac{A^2 H_1 G_0}{(E_1 - AF_1) - \frac{A^2 H_2 G_1}{(E_2 - AF_2) - \dots}} = 0. \quad (9)$$

Note that this is the same procedure used to obtain the continued fraction equation whose roots give the characteristic values of Mathieu's equation.

The bad curvature in the circular state causes the term -1 to appear in the expression for F_k . Note that the positive term in the expression for F_k is smallest when $n = 2$ and $m = 2$ (quadrupole fields). Hence the bad curvature has the greatest effect in this case. To examine this effect, F_k is rewritten in the form

$$F_k = 2 [\max(|n + 2km|, m) - d]. \quad (10)$$

By varying d , the effect of replacing bad curvature by good curvature, like that obtained in a cusp equilibrium, can approximately be examined. Figure 6(a) shows the path of $\hat{\omega}$ in the complex plane for $d = 1$ as A is varied from 0 to $\frac{1}{2}$, the threshold value given by Eq. (5). To obtain good accuracy for $0 < A < 0.2$ the continued fractions can be terminated at $k = \pm 5$, as stated in Ref. 5; but for $0.2 < A < 0.25$ the continued fractions must be taken out to $k = \pm 30$ to obtain 1% accuracy. The problem is that A plays two roles: increasing A tends not only to add stability through minimum- B , but also to increase the mode coupling. The complicated structure in Fig. 6(a) for $A > 0.2$ indicates that many modes are being coupled together.

As an estimate of the value of d to use in approximating the shape of the hypocycloid cusp, we propose the average curvature defined by

$$\left\langle \frac{1}{R_c} \right\rangle = \frac{1}{L} \int \frac{1}{R_c} ds = -\frac{\pi}{(24)^{1/2} r_s}, \quad (11)$$

$$\xi_r = \frac{r_s}{2} \sum_{k=-\infty}^{\infty} C_k \exp\{i[(n + 2km)\theta - (\hat{\omega} - 2km)\Omega t]\}, \quad (7)$$

where $\hat{\omega} = \omega/\Omega$. In the limit that $s_0 = \Omega r_s / [(\gamma p + B^2/\mu_0)/\rho]^{1/2} \ll 1$, the coefficients in Eq. (6) are given by simple formulas. (This condition requires that the rotation speed be much less than the speed of magnetosonic waves, a condition satisfied in experiments.)

$$\begin{aligned} F_k &= 2 [\max(|n + 2km|, m) - 1], \\ G_k &= |n + (2k + 1)m| - 1 - m \operatorname{sign}(n + 2km), \\ H_k &= |n + (2k - 1)m| - 1 + m \operatorname{sign}(n + 2km), \\ E_k &= \frac{(\hat{\omega} - 2km)^2}{|n + 2km|} + \frac{2(\hat{\omega} - 2km)}{n + 2km} + 1, \end{aligned} \quad (8)$$

where $\operatorname{sign}(x) = x/|x|$. The simplest way to solve this system of equations is to assume that $C_k = 0$ for $|k| > K$. For k positive, solve successively for C_k in terms of C_{k-1} starting with $k = K$ and ending with $k = 1$. For k negative, solve successively for C_k in terms of C_{k+1} starting with $k = -K$ and ending with $k = -1$. Then let K go to infinity to obtain continued fraction forms for C_1 and C_{-1} . Substitution in the $k = 0$ equation gives the dispersion relation

where the line integral is taken along the cusp surface from one tip to the next, ds is the differential arclength, L is the length along the surface from tip to tip, and R_c is the local radius of curvature. Hence we set $d = -\pi/(24)^{1/2} = -0.64$ to approximate the good curvature of the cusp. Figure 7(b) shows the path of $\hat{\omega}$ in the complex plane as a function of A . Note that a region of stability now appears between $A = 0.082$ and 0.112 , indicating that the stability properties of this system are quite sensitive to the choice of equilibrium shape. This sensitivity is hinted at in Ref. 5 where it was found that small windows of stability could be found by varying the radial equilibrium profile. Note also that the stability threshold is considerably lower than that predicted by Eq. (5), but that at larger values of A the increasing mode-coupling overwhelms the stabilizing effect and instability is again encountered. This is a general feature of the solutions of Eq. (6) as A is increased, even for $m = 3$ (hexapoles) and $m = 4$ (octopoles). In Ref. 5 it is stated that mode-coupling is unimportant for these two cases, but this is only partly true. It is true that stability is achieved at about the level predicted by Eq. (5), but if A increased further, instability reappears (at about $A = 0.18$ for $m = 3$ and $m = 4$). Thus the mode coupling is weaker for these two cases, but it is still important. This behavior is a consequence of the two roles of A mentioned before. For small values of A stability is increased as A is increased, but as A approaches a value near 0.18 , mode coupling acts to produce instability. It is interesting to note that experiments have been performed with $A > 0.25$ without any evidence of instability.¹⁰ This is another

indication that the circular analysis is inappropriate for this problem.

This state of affairs is both comforting and unsettling. On the one hand, it is probably unnecessary to worry about the lack of $n = 2$ stability with quadrupoles for the state shown in Fig. 1. The trouble is sensitive to the details of the equilibrium and can be made to go away by changing equilibrium parameters. However, the correct equilibrium could also be unstable; whether or not something like mode coupling plays a role can only be determined by finding the spectrum for an equilibrium of interest, like the unsavory geometry of Fig. 5. Note, however, that in Fig. 5 the curvature is good everywhere along the surface and that the restoring force at the cusp tips is very large because the radius of curvature goes to zero there. Hence the cusp equilibrium is expected to be more stable than the circular state.

It must be noted that the answer to this stability question has already been given with a different plasma model. In a series of hybrid simulations⁶ in which quadrupole fields

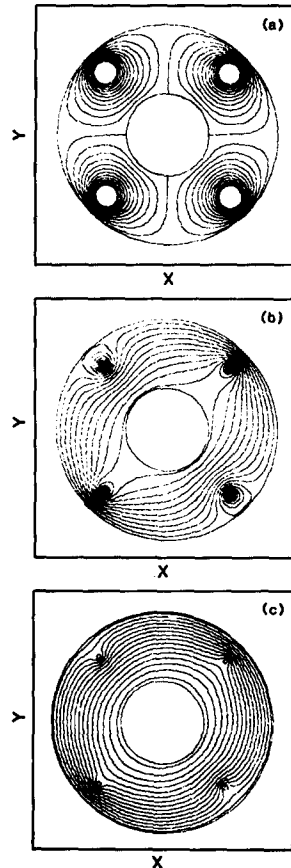


FIG. 7. Contours of helical flux are displayed for the conditions of the experiment of Ref. 4. (a) Helical flux for $\alpha = 0.001$ rad/cm and $I_q = 25$ kA. (b) Helical flux for $\alpha = 0.02$ rad/cm and $I_q = 10$ kA. (c) Helical flux for $\alpha = 0.04$ rad/cm and $I_q = 5$ kA.

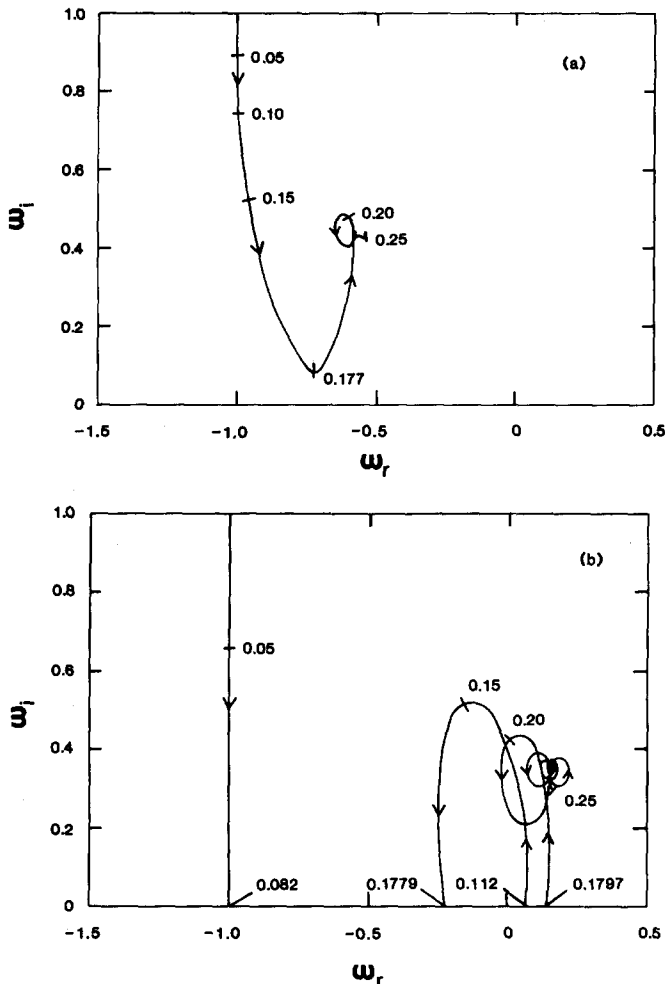


FIG. 6. The path of $\hat{\omega} = \omega/\Omega$ in the complex plane as A is varied is shown for two different equilibria. (a) This is a recalculation of Fig. 2 of Ref. 5 (circular equilibrium). It shows the path of $\hat{\omega} = \omega/\Omega$ in the complex plane as A is varied from 0.0 to 0.25 for the case of quadrupole fields and the $n = 2$ mode. The number of sideband frequencies included is 30 above and 30 below. Values of A are indicated at points along the path. (b) The path of $\hat{\omega}$ in the complex plane is displayed when the bad curvature has been artificially removed by setting d to the value appropriate to a cusp equilibrium, namely $d \approx -0.64$.

were imposed on an already spinning FRC, D. S. Harned observed that stabilization was achieved if B_m was large enough. It is difficult to compare the hybrid simulation with the MHD calculation because of differences in the models, but the simulation threshold is about 0.5–1.0 times the value given by Eq. (5) when both theories are applied to specific experiments. Strong deformation of the equilibrium shape, as in Fig. 4, was also observed. Presumably, an MHD calculation in the correct geometry would give a similar result. It should be noted, however, that the experimental thresholds are a factor of 2–5 below that given by Eq. (5).

IV. CONCLUSION

Results from experiments and simulations, as well as simple arguments based on the laws of hydrodynamics, show the rotating FRC's with excluded multipole fields are not approximately circular. Hence stability calculations based on a circular shape may be in error, especially when the results of these calculations depend critically on equilibrium details. Hybrid simulations⁶ show that quadrupole fields do indeed stabilize the rotational instability if the quadrupole fields are strong enough. Based on the simulations, Eq. (5) probably gives the right order of magnitude for the threshold.

There remains the problem of disagreement between the theories and the experiments. All of the quadrupole stabilization experiments have observed stabilization thresholds a factor of 2–5 below the threshold given in Eq. (5). A possible explanation for this discrepancy is that the multipole fields might slow the rotation so that a less stabilizing field is re-

quired. Since most experiments estimate the rotation frequency by observing the rotational instability, it is difficult to determine it when the instability is no longer present. In a series of experiments on FRX-C, however, the rotation was estimated³ by using the Doppler shift of light from Carbon V. It was observed that application of quadrupole fields did slow the rotation, presumably because of the viscosity of the deformed large-ion-orbit plasma. It is interesting to note that an octopole cusp is much more nearly circular than a quadrupole cusp. We might expect in this case to have little, if any, slowing down so that Eq. (5) might more closely predict the stabilization threshold. Both the lack of slowing down and a stability threshold more in agreement with Eq. (5) were observed in the octopole stabilization experiments on TRX-1.¹¹

Finally, there is the matter of the FRC experiments of Y. Nogi.⁴ In these experiments the straight quadrupole windings were changed to helical quadrupole windings with the result that the threshold current to achieve stabilization was a factor of 5–10 below Ishimura's threshold, given in Eq. (5). The equilibrium shape can be quite different in such a helical system because the open multipole field lines can become closed stellarator field lines. In particular, the cross-sectional shape could be very nearly circular with a small helical distortion, as indicated by the calculations presented in the Appendix. It may be that the resistance to rotation is even greater with a helical distortion than with a z -independent distortion because of coupling to the parallel viscosity.¹² This would reduce the apparent stabilization threshold.

ACKNOWLEDGMENTS

The authors wish to thank T. Ishimura for stimulating and useful discussions, and K. F. McKenna for the hologram displayed in Fig 3. One of us (R. L. Spencer) would like to thank the Hiroshima Institute for Fusion Theory for their hospitality during the time this work was begun.

This work was performed under the auspices of the United States Department of Energy.

APPENDIX: THE EFFECT OF HELICAL FIELDS

In this Appendix, we present a simple model that approximates an elongated FRC equilibrium with helical quadrupole fields, and we apply it to the experiment of Ref. 4. We assume an infinitely long system in the z direction; by so doing we ignore potentially important end effects that occur in experiments. The FRC and the theta-pinch coil are taken as conducting cylinders of radius a and c , respectively. Here we are assuming that the FRC rotates sufficiently fast to exclude the multipole fields from the region inside the separatrix. There is a uniform magnetic field $B_0 z$ for $a < r < c$. The quadrupole field is produced by wires wound on a cylinder of radius b ($a < b < c$) with pitch $\alpha = 2\pi/(\text{period length})$, and each conductor carries a current I_q . We assume vacuum fields in the region $a < r < c$ and solve for the scalar potential ϕ (from $\nabla^2 \phi = 0$) with helical coordinates r and $u = \theta - \alpha z$. Then, we find the vector potential \mathbf{A} from the relation $\nabla \times \mathbf{A} = \nabla \phi$ and define the flux function $\psi = \alpha r A_\theta$, following Ref. 13. We find

$$\psi = \frac{B_0 \alpha r^2}{2} + 8B_q r(\alpha b)^2 \sum_{p=0}^{\infty} \frac{\cos Nu}{I'_{Nc} K'_{Na} - I'_{Na} K'_{Nc}} \times \begin{cases} (I'_{Nc} K'_{Nb} - I'_{Nb} K'_{Nc})(I'_N K'_{Na} - I'_{Na} K'_N), \\ a < r < b, \\ (I'_{Na} K'_{Nb} - I'_{Nb} K'_{Na})(I'_N K'_{Nc} - I'_{Nc} K'_N), \\ b < r < c, \end{cases} \quad (\text{A1})$$

where $B_q = \mu_0 I_q / 2\pi b$ and $N = 2(2p + 1)$. In Eq. (A1) I'_N means $I'_N(N\alpha r)$ and I'_{Nx} means $I'_N(N\alpha x)$; similarly for K'_N and K'_{Nx} . We present in Fig. 7 helical flux contours computed from Eq. (A1) for values of α and I_q used in the experiment of Ref. 4. In Fig. 7 we took $a = 3$ cm, $b = 6.5$ cm, $c = 8$ cm, and $B_0 = 9$ kG, the experimental values in Ref. 4. We observe from Fig. 7(c) that closed flux surfaces surround the FRC for sufficient pitch angle α . This is in contrast to the straight quadrupole case of Fig. 7(a) where all of the field lines outside the FRC are open. A transition between open and closed field lines is made near the case of Fig. 7(b). For a value of I_q corresponding to the stability threshold of Eq. (5), and for the experimental conditions of Ref. 4, this transition occurs for $ab \simeq 0.75$. If a lower value of I_q is sufficient to stabilize the rotational instability, as suggested by the experimental data,⁴ then this transition occurs at smaller values of ab , e.g., $ab = 0.13$ for Fig. 7(b). The presence of nearly circular flux surfaces, such as those in Fig. 7(c), ensures that the equilibrium shape of the FRC in the presence of helical fields is essentially unchanged from the shape before application of the helical fields. In particular, there will be no cusp points like those that occur in the straight quadrupole case. Furthermore, the presence of closed field lines outside the FRC should be beneficial for FRC confinement since there is no gradual opening of the field lines inside the separatrix. This is in contrast to the straight quadrupole case where the FRC is eaten away as the quadrupole field diffuses into the separatrix, an effect that may become significant if the rotation slows down in time.³ The improved confinement of plasma on open field lines suggested by the flux surfaces of Fig. 7(c) should also be beneficial, e.g., density gradients near the separatrix should be reduced and impurity and neutral in-fluxes should also be reduced as wall contact is suppressed.

Finally, even though the distortion from circularity is small it could have important consequences because it forces the coupling of rotational and axial motion. This could allow the rotation to be damped by the parallel ion viscosity, reducing the threshold for stabilization. In this regard, it is interesting to note that in Nogi's experiment, as the pitch of the winding was increased, the time of application of the helical fields was made earlier and earlier. Hence some of the reduction in the current needed to stabilize the mode could be caused by applying the fields at earlier times when the plasma has presumably not had a chance to spin up very much.

¹S. Okada, Y. Kawakami, K. Takeuchi, T. Minato, M. Tanjyo, Y. Ito, M. Kako, S. Ohi, S. Goto, T. Ishimura, and H. Ito, in *Proceedings of the*

Fourth US-Japan Workshop on Compact Toroid Research, Osaka, Japan, October 1982 (Osaka University, Osaka, Japan, 1982), p. 104.

²A. L. Hoffman, J. T. Slough, and D. G. Harding, in Ref. 1, p. 132.

³R. E. Siemon, W. T. Armstrong, D. C. Barnes, R. R. Bartsch, R. E. Chrien, J. C. Cochrane, W. Hugrass, R. W. Kewish, Jr., P. L. Klinger, H. R. Lewis, R. K. Linford, K. F. McKenna, R. D. Milroy, D. J. Rej, J. L. Schwarzmeier, C. E. Seyler, E. G. Sherwood, R. L. Spencer, and M. Tuszewski, submitted to *Fusion Technol.*

⁴Y. Nogi, S. Shimamura, Y. Shimada, T. Ikawa, and H. Yoshikawa, in the *Proceedings of the Fifth US-Japan Workshop on Compact Toroid Research*, Princeton, NJ, February 1984 (Princeton Plasma Physics Laboratory, Princeton, NJ, 1985), p. 141.

⁵T. Ishimura, *Phys. Fluids* **27**, 2139 (1984).

⁶D. S. Harned, *Phys. Fluids* **27**, 554 (1984).

⁷D. S. Harned (private communication).

⁸R. L. Spencer, *Phys. Fluids* **23**, 1691 (1980).

⁹J. Berkowitz, in *Proceedings of the 2nd UN Conference on the Peaceful Uses of Atomic Energy*, Geneva, Switzerland, 1958 (IAEA, Vienna, 1958), Vol. 31, p. 171.

¹⁰R. E. Chrien (private communication).

¹¹A. L. Hoffman, J. T. Slough, and D. G. Harding, *Phys. Fluids* **26**, 1626 (1983).

¹²J. M. Dawson (private communication).

¹³A. I. Morozov and L. S. Solovév, in *Reviews of Plasma Physics*, edited by M. A. Leontovich (Consultants Bureau, New York, 1969), Vol. 2, p. 1.